The 2010 IEEE/RSJ International Conference on
Intelligent Robots and Systems
October 18-22, 2010, Taipei, Taiwan

Terramechanics-based Propulsive Characteristics of Mobile Robot Driven by Archimedean Screw Mechanism on Soft Soil

Kenji Nagaoka, Masatsugu Otsuki, Takashi Kubota and Satoshi Tanaka

Abstract— **This paper describes the mathematical modeling and the propulsive characteristics of a novel robot driven by Archimedean screw mechanisms, named Screw Drive Rover. For secure locomotion on soft soil, the proposed rover would become one of the good solutions because of its robustness to slipping and getting stuck in the soil. Furthermore, the rover is expected to move in various directions by using the dual screw units. However, the interaction between such screw unit and the surrounding soil is quite complicated and remains undefined. So, this paper attempts to model the tractive effort of the rover on the soil. The mathematical modeling is newly developed based upon terramechanics, addressing soil-vehicle interactive mechanics. Finally, the validity of the proposed model is demonstrated by simulation analyses.**

I. INTRODUCTION

Robotic exploration by mobile rovers has received attention worldwide toward the achievement of progressive space missions. Recently, the Mars Exploration Rovers (MERs) operated by NASA have performed impressive exploration activities on Mars. The MERs employ six wheels for traveling over the martian surface, and until now these rovers have acquired scientific findings for more than 6 years. Meanwhile, the Spirit rover, which is one of the two MERs, has been mired in a martian version of quicksand since May 2009 [1]. Since then, mission engineers have investigated how the Spirit rover might extricate itself from the sand trap. However, on January 2010, it was announced NASA eventually turned off its extrication. This determinately indicates a limitation of wheeled locomotion on soft soil such as lunar regolith. Therefore, advanced gears or improved wheels must be newly developed to cope with such a difficult terrain.

The authors have proposed a mobile robot driven by an Archimedean screw mechanism, specialized for traveling on soft soil. This screw mechanism is used as a drilling device to remove subsoils and penetrate deep into the ground. In accordance with this, the rover is expected to be robust to slipping and getting stuck in the soil since the mechanism can forge ahead even if it is buried in the soil. In addition, inclined screw blades lead to movement in various directions. Compared to a track, its structural simplicity has a decided advantage in unmanned rovers.

This work was supported by Japan Aerospace Exploration Agency.

K. Nagaoka is with Department of Space and Astronautical Science, The Graduate University for Advanced Studies (Sokendai), Yoshinodai 3-1-1, Chuo-ku, Sagamihara 2525210, Japan nagaoka@nnl.isas.jaxa.jp

M. Otsuki, T. Kubota and S. Tanaka are with Institute of Space and Astronautical Science, Japan Aerospace Exploration Agency, Yoshinodai 3-1-1, Chuo-ku, Sagamihara 2525210, Japan {otsuki,kubota}@isas.jaxa.jp, tanaka.satoshi@jaxa.jp

Such a spiral structure has been attractive to humans since ancient times [2]. In particular, the Archimedean screw mechanism is well known as a screw-pump for transferring water [3]. On the other hand, it has been also applied to land and amphibious vehicles since around the 19th century [4]. The vehicles provide high trafficability in a difficult surface consisting of snow, ice, mud, marsh or sand. So far, a small number of experimental studies on the screw mechanism or the vehicle have been reported [5]–[7]. Dugoff et al. [6] especially examined the characteristics between translatory traction and slip of a single screw rotor by varying screw geometry, load and velocity. But its applicable scope would be confined to straight movement, and also a study on a soil-screw interaction is lacking. Consequently, the vehicles' synthetic trafficability over the soil is less well understood. For this reason, a new challenge of comprehending the soil-screw interaction comes for a practical application of the screw mechanism. Likewise, there have been several robots using a spiral, for instance, an in vivo robot for laparoscopy [8], a robotic endoscope [9] or a swimming micro-machine [10]. In vivo and underwater robots move by contact with viscoelastic biological tissue and incompressible viscous fluid, respectively. Although these are equipped with the spiral mechanisms similar to the screw for locomotion, their targeted environments are quite different from the soil. Understandably, their interactive models essentially differ from the proposed rover's one as well. Hence, individualistic modeling is practically required for each application.

This paper focuses on the derivation of the novel soil-screw interaction model. As the first step, this paper addresses the interaction model based upon conventional terramechanics studies [11], [12]. In this paper, unlike the conventional wheel or track models, three-dimensional screw helical motion is newly considered. Then, characteristics of the developed model are also elaborated by simulations.

II. SCREW DRIVE ROVER SYSTEM

A. System Configuration and Ideal Mobility

The author has proposed and developed a novel rover using the Archimedean screw units, named Screw Drive Rover. The rover is composed of a main body, hinge legs, and sinistral and dextral screw units. As for the screw unit, helical screw blades are attached along cylindrical shafts. The screw blades set to be wound N-times around the shafts. Further, the rover can improve its attitude stability by driving the hinge legs in synchronization. In principle, the screw units can propel the rover in soil. Consequently, the rover is robustness to slipping and getting stuck. Employing the two

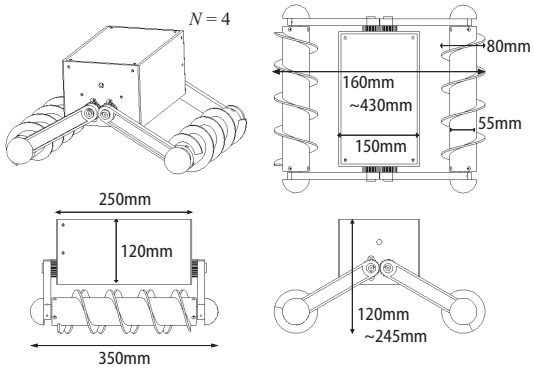

(a) 3D CAD drawing

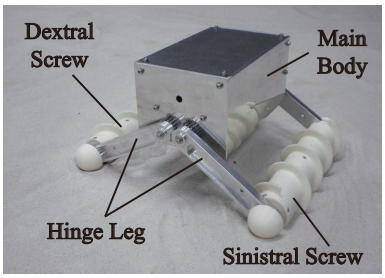

(b) Prototype overview

Fig. 1 Schematic of Screw Drive Rover

screw units also enables the rover to maneuver on soil.

To discuss the mobility performance of the rover, the authors have first analyzed the ideal kinematic model [13]. The model is defined by just skin friction acting on the screw blades and the cylindrical shafts. According to the model analysis, the modeled rover achieves various locomotion trajectories by using the two screw units. Of particular note is that such diverse maneuverability has been demonstrated in the real screw vehicles. Meanwhile, given that the rover travels by only the skin frictions, the ideal moving paths traced by the rover are not consistent with experimental ones. Rather, a propulsive force in normal direction to the friction on the screw blades is more suitable for the maneuver. This can be also estimated from rut recovery on the surface. Therefore, modeling a soil-screw interaction is required to examine the propulsive characteristics of the rover.

B. Review of Preliminary Traveling Tests on Sand

Prior to the detailed theoretical discussion, labptaroty tests have been conducted on the Screw Drive Rover prototype to grasp its practical trafficability. Schematic of the rover is shown in Fig. 1. The screw slope angles are designed to be 16 degrees (N=4). The total system weights 6.4 kilograms without circuits and batteries, and the dimension is illustrated in Fig. 1(a). Two motors are separately built in the screw units respectively, and a motor inside the body is carried to drive the hinge legs. Typical maneuvers by the traveling tests are shown in Fig. 2. From these results, it is confirmed the proposed rover is able to realize multi-directional locomotion by the two screw units.

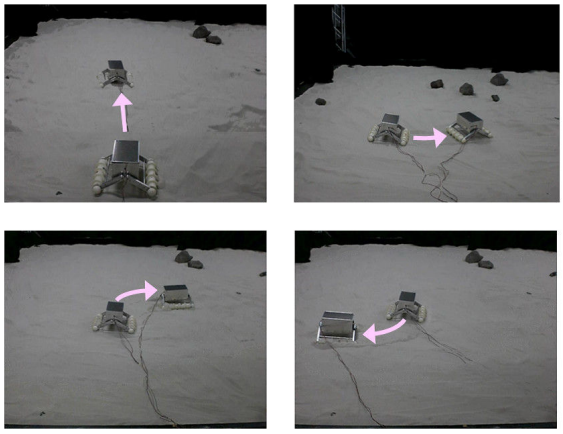

Fig. 2 Empirical maneuvers of the prototype

C. Challenge and Motivation

Because the ideal model does not include the interaction, the development of the model with the soil mechanics would appear as a challenge. In this paper, the modeling of the soil-screw interactive mechanics is conducted based on terramechanics contributions [11], [12]. Then, the simulated tractive performances of the Screw Drive Rover are analytically discussed. Particularly, the locomotion model would become a nonholonomic system, and therefore, the modeling is of considerable significance for the achievement of desired movement.

III. MODELING OF SOIL-SCREW INTERACTION

A. Preliminary

The motion states of the Screw Drive Rover are preliminarily defined. Absolute coordinate system $\Sigma_O\{X, Y, Z\}$ is set as illustrated in Fig. 3. The modeling assumes a family of soil-screw moving together as one body. Further to this, the screw model technically depends on its winding direction but subsequent definitions and formulas can be essentially regarded as common expressions. Therefore, unified expressions are described for each screw unit unless stated otherwise.

B. Screw Geometric Definitions

First, the screw pitch and the slope angle are defined as p and η, respectively. These values are constant and represented at the midpoint between the cylinder surface and the screw blade edge. Here, p and η satisfy the following relation.

$$p = \pi (r + r_1) \tan \eta \tag{1}$$

where r_1 is the screw cylinder radius, r_2 is the screw blade's height and r is also defined as $r = r_1 + r_2$. Here, the screw length b is defined as $b = N \cdot p$.

The screw blade surface area, dA, at micro region $d\theta$ from the screw winding angle θ, can be approximated as follows.

$$dA(\theta) = \pi (r^2 - r_1^2) \cdot d\theta \tag{2}$$

The locomotion is basically governed by forces on dA.

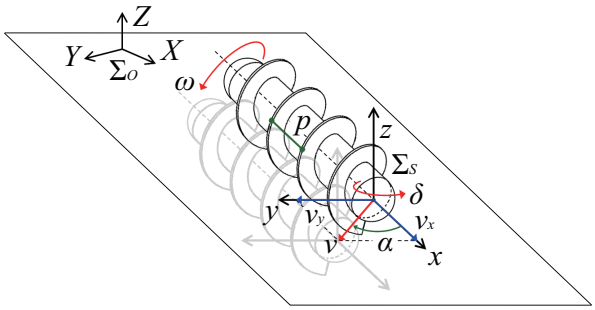

Fig. 3 Kinematics model of the screw unit

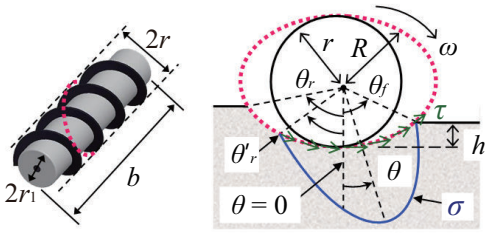

Fig. 4 Soil-screw interaction

C. Slip in Motion

The screw fixed coordinates $\Sigma_S\{x, y, z\}$ is first set to be the right-handed coordinate system with the x and y axis in the longitudinal and vertical directions of the screw unit. Fig. 3 shows the kinematic model of the screw unit. Σ_S is defined as the rotating frame to Σ_O, which rotates around Z axis by δ. Basically, robotic locomotion on soil is accompanied by slip due to soil compaction and failure. The slip in x axis, s_x, is defined as follows [6], [12].

$$s_x = \begin{cases} \frac{p\omega/2\pi - v_x}{p\omega/2\pi} & \text{if} \quad |p\omega/2\pi| \geq |v_x| \\ \frac{p\omega/2\pi - v_x}{v_x} & \text{otherwise} \end{cases} \tag{3}$$

where ω is the screw angular velocity, v_x is the velocity component in x direction, $0 \leq s_x \leq 1$ under a driving state and $-1 \leq s_x \leq 0$ under a braking state. This paper employs s_x to evaluate the kinematic state.

D. Direction of Locomotion

Given the velocity vector v in Σ_S, the angle between v and the x axis can be defined as slip angle α [15]. By the velocity components v_x and v_y in Σ_S, α is expressed as follows.

$$\alpha = \tan^{-1}\left(v_y / v_x\right) \tag{4}$$

Likewise, v_x and v_y can be also written by

$$v_x = \frac{p\omega\,(1 - s_x)}{2\pi}, \quad v_y = \frac{p\omega\,(1 - s_x)}{2\pi}\tan\alpha \tag{5}$$

E. Mathematical Formulations of Contact Stresses

1) Normal Stress: The relationship between normal stress σ and sinkage h is one of the significant subjects in terramechanics. Note that the traditional terramechanics equations discussed below are semi-empirical models based on reacted soil behavior. The normal stress distribution of soil beneath a rolling circular object, such as a rigid wheel or the screw unit, is defined as follows [11], [12].

$$\sigma(\theta) = \begin{cases} \sigma_m \Theta_1^n & \text{if} \quad \theta_m \leq \theta \leq \theta_f \\ \sigma_m \Theta_2^n & \text{otherwise} \end{cases} \tag{6}$$

and also,

$$\Theta_1(\theta) = \cos\theta - \cos\theta_f \tag{7}$$

$$\Theta_2(\theta) = \cos\left[\theta_f - \frac{\theta - \theta'_r}{\theta_m - \theta'_r}\left(\theta_f - \theta_m\right)\right] - \cos\theta_f \tag{8}$$

$$\sigma_m = \left(k_c/b + k_\phi\right)R^n \tag{9}$$

where θ is the screw angle ($\theta'_r \leq \theta \leq \theta_f$), θ'_r (≤ 0) is the effective exit angle, θ_f (≥ 0) is the entry angle, θ_m is the specific wheel angle at which the maximized normal stress occurs, b is the screw's longitudinal length, n is sinkage exponent, and k_c and k_ϕ are pressure-sinkage moduli regarding cohesion and internal friction, respectively. Let R be the elliptic distance as illustrated in Fig. 4, and will be defined later on. In addition, relational angle expressions can be given by the following equation [12], [14].

$$\theta_f = \cos^{-1}(1 - h/r) \tag{10}$$

$$\theta_m = (c_1 + c_2 s_x)\,\theta_f \tag{11}$$

where c_1 and c_2 are coefficients depending on the soil-screw interaction.

The conventional study in terramechanics is basically premised on $|\theta_r| \leq |\theta_f|$ for the expression of σ beneath a rigid wheel. In the case of the screw unit, however, $|\theta_f| \leq |\theta_r|$ has been observed through the traveling tests by the authors. This implies the reaction force from discharging soil is too small, and therefore, the stress distribution satisfying $|\theta_f| \leq |\theta_r|$ is obtained. Therefore, this paper assumes $|\theta_f| \leq |\theta_r|$ by means of a transformation of θ_r to θ'_r. θ'_r achieving $|\theta'_r| \leq |\theta_f|$ is given as follows.

$$\theta'_r = -c_3\theta_f \tag{12}$$

where c_3 (≤ 1) is a positive angle coefficient.

The screw unit provides a elliptic cross section for discussing the normal and the shear stresses with angle θ as illustrated in Fig. 4. In wheels, while the soil is sheared in elliptic trajectory when a wheeled vehicle steers, the common formula of the normal stress is applicable [15]. Hence, this paper also employs the unified normal stress distribution (6).

2) Shear Stress: The shear stress τ of soft soil is formulated as follows [17].

$$\tau(\theta) = \tau_{\max} \cdot \left(1 - \exp^{-j/K}\right) \tag{13}$$

$$\tau_{\max}(\theta) = c + \sigma\tan\phi \tag{14}$$

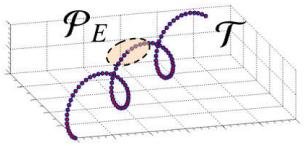

(a) Trajectories of screw blade and soil displacement

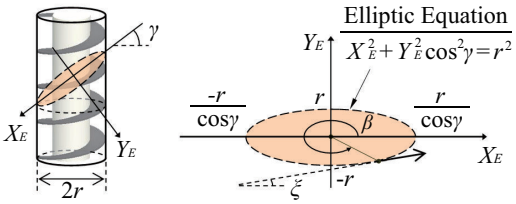

(b) Soil shearing ellipse

Fig. 5 Elliptic trajectory of soil shearing

where $\tau_{\max}$ is shear strength, ϕ is soil internal friction angle, c is soil cohesion, j is soil displacement and K is shear deformation modulus.

3) Shear Displacement of Soil: Unlike the traditional approaches, this paper takes into account three-dimensional soil transportation. In general, the soil between the screw blade is regarded as one body with the screw blade. From this point of view, it can be assumed that the soil shear stress occurs along the outermost radius of the screw blade. Consequently, the expression of the screw's helical trajectory is needed to model the soil thrust of τ. This paper provides the screw motion trajectory in Σ_O, $\mathcal{T}(X, Y, Z)$, by the following expression.

$$\mathcal{T} = \begin{pmatrix} r\cos\theta\sin\delta + V_X t + X_0 \\ r\cos\theta\cos\delta + V_Y t + Y_0 \\ r\sin\theta + Z_0 \end{pmatrix}^T \tag{15}$$

and also,

$$\begin{cases} V_X = v_x\cos\delta + v_y\sin\delta \\ V_Y = -v_x\sin\delta + v_y\cos\delta \end{cases} \tag{16}$$

Then, the trajectory of the soil shearing is defined by angle γ $(= \pi/2 - \eta)$ as illustrated in Fig. 5. This trajectory $\mathcal{P}_E(X_E, Y_E, Z_E)$ basically traces an ellipse. In the screw fixed elliptic coordinates $\Sigma_E\{X_E, Y_E, Z_E\}$, $\mathcal{P}_E$ can be derived by β or θ $(= \beta - 3\pi/2)$.

$$\mathcal{P}_E = \begin{pmatrix} \frac{r}{\cos\gamma}\cos\beta \\ r\sin\beta \\ 0 \end{pmatrix}^T = \begin{pmatrix} \frac{-r}{\cos\gamma}\sin\theta \\ r\cos\theta \\ 0 \end{pmatrix}^T \tag{17}$$

The tangential equation at a certain point $(x_a, -y_a)$ on $\mathcal{P}_E$ is also represented as follows.

$$\frac{x_a}{r^2\sec^2\gamma}\cdot X_E + \frac{y_a}{r^2}\cdot Y_E = 1 \tag{18}$$

where x_a and y_a are positive values, and the sinkage is assumed to be less than r. Substituting (17) into (18), the above equation can be eventually simplified as follows.

$$y_a = -\frac{\cos\gamma}{\tan\beta}\cdot x_a + \frac{r\cos\gamma}{\sin\beta} \tag{19}$$

Accordingly, the inclination angle of the tangent, ξ, can be written as follows.

$$\xi = \tan^{-1}(-\cos\gamma\cdot\cot\beta) = \tan^{-1}(\cos\gamma\cdot\tan\theta) \tag{20}$$

Furthermore, the ellipse radius R is formulated as a function of θ by

$$R(\theta) = r\sqrt{\cos^2\theta + \sin^2\theta\cdot\sec^2\gamma} \tag{21}$$

Thus, j can be ultimately defined as follows.

$$j(\theta) = \oint_{\mathcal{L}} v_j\, dt \tag{22}$$

and also,

$$\mathcal{L} = \mathcal{T} + \mathcal{P}_O \tag{23}$$

$$\mathcal{P}_O = \begin{pmatrix} -r\sin\theta\cdot\sin(\delta+\gamma) \\ -r\sin\theta\cdot\cos(\delta+\gamma) \\ -r\sec\gamma\cdot\cos\theta \end{pmatrix}^T \tag{24}$$

where $\mathcal{L}$ is the trajectory of the displaced soil in Σ_O and v_j is the relative soil displacement velocity along $\mathcal{L}$. Moreover, $\mathcal{P}_O$ gives a transformation from $\mathcal{P}_E$, transforming their coordinates $\Sigma_E \to \Sigma_O$. In light of (5), the time derivative of $\mathcal{L}$ is given as follows.

$$\begin{aligned} \frac{d}{dt}\mathcal{L} &= \frac{d}{dt}(\mathcal{T} + \mathcal{P}_O) \\ &= \begin{pmatrix} \frac{p(1-s_x)}{2\pi} - r\cos\theta\sin\gamma \\ \frac{p(1-s_x)}{2\pi}\tan\alpha - r(\sin\theta + \cos\theta\cos\gamma) \\ r\cos\theta + \frac{r}{\cos\gamma}\sin\theta \end{pmatrix}^T \cdot\omega \\ &= \begin{pmatrix} \mathcal{L}_{v_{jx}} & \mathcal{L}_{v_{jy}} & \mathcal{L}_{v_{jz}} \end{pmatrix}\cdot\omega \end{aligned} \tag{25}$$

where δ and $\dot{\delta}$ are assumed to be zero.

Therefore, (22) can be finally expressed as follows.

$$j(\theta) = \oint_{\mathcal{L}} v_j\cdot dt = \int_{\theta}^{\theta_f}\sqrt{\mathcal{L}_{v_{jx}}^2 + \mathcal{L}_{v_{jy}}^2 + \mathcal{L}_{v_{jz}}^2}\, d\theta \tag{26}$$

4) Stationary State of Dynamic Sinkage: Yamakawa et al. [18] has investigated the dynamic sinkage of a wheel, and concluded that the sinkage reaches a stationary state under constant slip. In [19], similar slip-sinkage characteristics have been also reported with experimental results. On the basis of these literatures, it is estimated that the stationary sinkage is proportional to the slip. The proportionality factor depends on both the wheel and the soil. Hence, this paper assumes the simplified relationship as follows.

$$h = h_0 + c_4 s_x \tag{27}$$

where h_0 is static sinkage before driving, c_4 is a positive coefficient. This enables as to simulate the relativity of the slip and the sinkage.

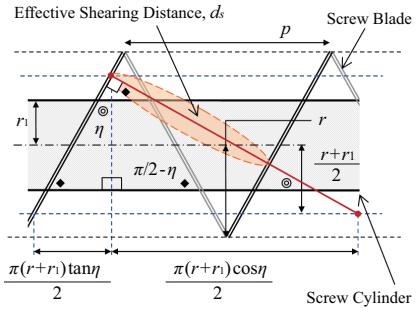

(a) Illustration of effective shearing distance

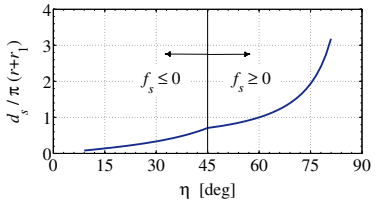

(b) Parametric analysis of d_s depending on η

Fig. 6 Effective distance of soil shearing

5) Effective Factor of Soil Shearing Distance: The effective distance of the soil shearing, d_s, is geometrically constrained by η and p as illustrated in Fig. 6(a). To evaluate the distance, the effective factor f_s is given as follows.

$$f_s = \frac{p}{r_1} - \frac{\pi\,(r + r_1)\,(\tan\eta + \cot\eta)}{2r_1} \tag{28}$$

Thus, d_s is maximized with the positive f_s. Contrary to this, when f_s is negative, d_s is confined to the inter-screw area. The positive f_s obviously appears at 45deg $\le \eta \le$ 90deg. Consequently, d_s can be introduced as follows.

$$d_s = \begin{cases} \frac{\pi(r+r_1)\tan\eta}{2\sin\eta} & \text{if} \quad f_s \ge 0 \\ \frac{\pi(r+r_1)\tan\eta}{2\cos\eta} & \text{otherwise} \end{cases} \tag{29}$$

Fig. 6(b) depicts the characteristics of d_s pertaining to η. According to this, d_s is strongly governed by η.

IV. SYNTHETIC LOCOMOTION MODEL

A. Integrated Tractive Efforts

In accordance with the developed model, this section introduces the tractive efforts as synthetic models. The integrated tractive effort in x direction of the Screw Drive Rover is defined as F_x and is calculated as follows.

$$F_x = \sum \operatorname{sgn}(\omega)\, F \cos\eta \tag{30}$$

$$F = \iint (\tau\cos\xi - \sigma\sin\xi)\; dA\, d\theta \tag{31}$$

where $\sum$ denotes the summation of the screw units. Let the integral region be determined based on d_s. Here, because the tractive efforts are evaluated by whole integration, (31) can be modified as follows.

$$F = b \cdot R\sin\eta \int_{\theta_r'}^{\theta_f} (\tau\cos\xi - \sigma\sin\xi)\; d\theta \tag{32}$$

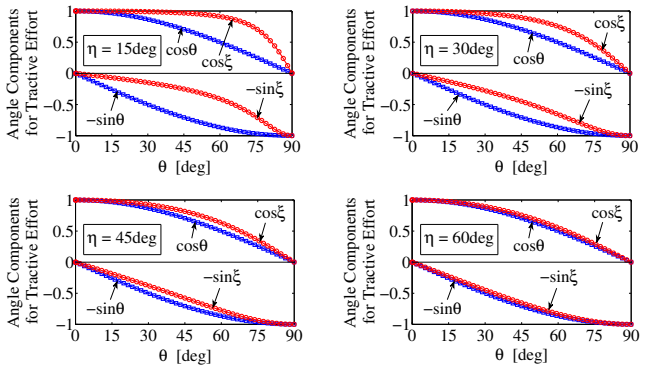

Fig. 7 Angle components for tractive effort of stresses on circular and elliptic surfaces along angles

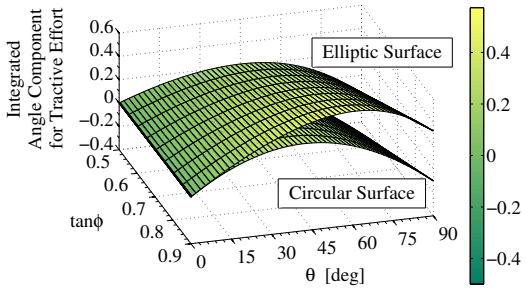

Fig. 8 Integrated angle components for tractive effort of stresses on circular and elliptic surfaces along angles

Likewise, that in y direction, F_y, is computed by

$$F_y = \sum \operatorname{sgn}(\omega)\, F \sin\eta \tag{33}$$

where the body rotation δ is assumed to be ignored in primary analysis, giving $\delta = \dot{\delta} = 0$.

B. Emphasis of Stresses Acting on Elliptic Surface

In the proposed model, τ acts as $\tau\cos\xi$ and σ as $-\sigma\sin\xi$ for tractive efforts in x direction. On the contrary, τ acts as $\tau\cos\theta$ and σ as $-\sigma\sin\theta$ for a wheel. The active angle component of each stress for the tractive effort is plotted in Fig. 7. These results indicate the elliptic surface has an advantage over the circular one with smaller η. Further, Fig. 8 depicts the ideal integrated angle components, $\int_0^{\theta}(\tan\phi\cos\theta - \sin\theta)\; d\theta$ and $\int_0^{\xi}(\tan\phi\cos\xi - \sin\xi)\; d\xi$. Here, the integrating components assume the available maximum shear stress of cohesionless soil in (13), which is $\tau = \sigma\tan\phi$. The simulated plots indicate the elliptic surface works better.

V. SIMULATION ANALYSIS

A. Fundamental Parameter Conditions

Through the simulations, the tractive effort F_x is calculated when Screw Driver Rover travels in a straight line. This provides δ=0 and α=0 as kinematic constraints. By reference to the experiments by Dugoff et al. [6], s_x is similarly set to be a variable parameter. With respect to the kinematic and geometric conditions, the nominal parameters are set: N=4, η=5~30deg, r_1=0.035m, r_2=0.015m,

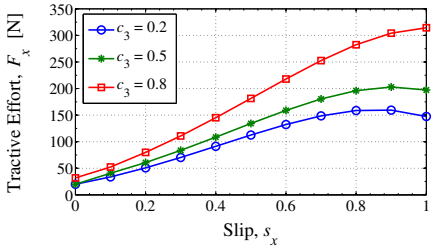

(a) With varying c_3, η=16deg and c_4=0.03

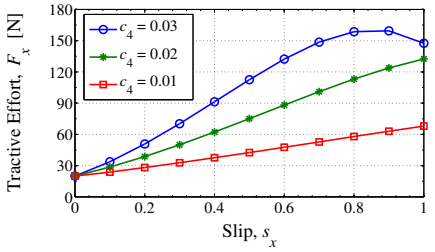

(b) With varying c_4, η=16deg and c_3=0.2

Fig. 9 Simulated tractive effort and slip of Screw Drive Rover model with varying parameters

h=0.01~0.04m (h_0=0.01m), ω=$\pm\frac{\pi}{2}$rad/s. Likewise, according to the experimental data targeting the sampled lunar soil [20] and the previous works [16], each soil parameter is set: K=0.018m, c=0.17kPa, ϕ=35deg, c_1=0.4, c_2=0.15, c_3=0.2~0.8, c_4=0.01~0.03, n=1.0, k_c=1379N/m^{n+1} and k_ϕ=814.4kN/m^{n+2}.

B. Result and Discussion

Fig. 9 plots the simulation results performed by the proposed model. These results show the predicted tractive effort F_x with the slip s_x. According to these, it is confirmed F_x increases with an increase in s_x in most situations. This typical tendency was observed in the past experiments [6], and therefore, this confirms the validity of the model. Fig. 9(a) shows the tendency that an increase of the exit angle θ_r' introduces larger F_x. Although this indicates an increase of contact surface is significant, c_3 is unlikely to have a significant impact on F_x, compared to η. Moreover, Fig. 9(b) depicts the tendency that the sinkage h exerts an effect on F_x. Better understanding of the dynamic sinkage is needed in the future work. On the whole, the ratio of the sinkage and the radius h/r becomes a key factor in the light of Fig. 8. An appropriate control of h/r is the most important technique for the enhancement of mobility performance of the Screw Drive Rover on the soft soil. So that the rover always generates positive tractive efforts, the design of η also becomes another important factor.

VI. CONCLUSIONS

This paper presents the novel robot system using the Archimedean screw mechanism and its new mathematical model for traveling on soil. The modeling is developed based on terramechanics with the screw geometry. In particular, the soil shearing ellipse or trajectory is formulated as three-dimensional motion. Such an attempt will contribute the locomotion control, and even understanding the soil behavior. In this paper the traction-generating mechanism of the screw unit is explained with the soil shear. Likewise, the parametric analysis of the model enables one to improve the mechanical design. As for future works, experimental validation is required by the prototype. Some feedback from experimental results to the model should be also conducted to control the rover based on the model. In addition to these, the skin frictions visibly occur on the screw surface. That is, both the frictions and the developed model are actually needed to be combined for precise control. The fusion is the next important stage in this study.

REFERENCES

[1] R.A. Kerr, Mars Rover Trapped in Sand, But What Can End a Mission?, *Science*, vol. 324, no. 5930, 2009, p. 998.

[2] C.A. Pickover, Mathematics and Beauty: A Sampling of Spirals and 'Strange' Spirals in Science, Nature and Art, *Leonardo*, vol. 21, no. 2, 1988, pp. 173-181.

[3] T. Koetsier and H. Blauwendraat, "The Archimedean Screw-Pump: A Note on its Invention and the Development of the Theory", *in Proc. Int. Symp. History of Machines and Mechanisms 2004*, Cassino, Italy, 2004, pp. 181-194.

[4] T.J. Wells, *Improvement in the Manner of Constructing and of Propelling Steamboats, Denominated the "Buoyant Spiral Propeller"*, U.S. Patent, USA, no. 2400, Dec. 23rd, 1841.

[5] S.J. Knight, E.S. Rush and B.G. Stinson, Trafficability Tests with the Marsh Screw Amphibian, *J. Terramech.*, vol. 2, no. 4, 1965, pp. 31-50.

[6] H. Dugoff and I. Ehrlich, Model Tests of Buoyant Screw Rotor Configurations, *J. Terramech.*, vol. 4, no. 3, 1967, pp. 9-22.

[7] L. Ju et al., "Experimental Results of a Novel Amphibian Solution for Aquatic Robot", *in Proc. 2010 IEEE Int. Conf. Rob. Autom.*, Anchorage, AK, USA, 2010, pp. 2261-2266.

[8] M.E. Rentschler et al., Modeling, Analysis, and Experimental Study of In Vivo Wheeled Robotic Mobility, *IEEE Trans. Rob.*, vol. 22, no. 2, 2006, pp. 308-321.

[9] M. Shikanai et al., "Development of a Robotic Endoscope that Locomotes in the Colon with Flexible Helical Fins", *in 31st Annual Int. Conf. IEEE/EMBS*, Minneapolis, MN, 2009, pp. 5126-5129.

[10] A. Yamazaki et al., Three-Dimensional Analysis of Swimming Properties of a Spiral-Type Magnetic Micro-Machine, *Sens. Act. A*, vol. 105, no. 1, 2003, pp. 103-108.

[11] M.G. Bekker, *Introduction of Terrain-Vehicle Systems*, University of Michigan Press, MI; 1969.

[12] J.Y. Wong, *Theory of Ground Vehicles (Third Edition)*, John Wiley & Sons, NY; 2001.

[13] K. Nagaoka, M. Otsuki, T. Kubota and S. Tanaka, "Development of Lunar Exploration Rover Using Screw Propulsion Units: Note on Dynamic Behavior and Moving Direction Control", *in 19th Workshop on JAXA Astrodyn. Flight Mech.*, Kanagawa, Japan, 2009, pp. 143-148.

[14] O. Onafeko and A.R. Reece, Soil Stresses and Deformations beneath Rigid Wheels, *J. Terramech.*, vol. 4, no. 1, 1967, pp. 59-80.

[15] D.A. Crolla and A.S.A. El-Razaz, A Review of the Combined Lateral and Longitudinal Force Generation of Tyres on Deformable Surfaces, *J. Terramech.*, vol. 24, no. 3, 1987, pp. 199-225.

[16] K. Iagnemma and S. Dubowsky, *Mobile Robots in Rough Terrain*, Springer, Germany; 2005.

[17] Z.J. Janosi and B. Hanamoto, "The Analytical Determination of Drawbar Pull as A Function of Slip for Tracked Vehicle", *in 1st Int. Conf. Terrain-Vehicle Sys.*, Turin, Italy, 1961, pp. 707-736.

[18] J. Yamakawa, O. Yoshimura and K. Watanabe, Development of Tire Model on Dry Sand by Model Size Experiment (First Report), *Trans. Soc. Automotive Eng. Jpn.*, vol. 39, no. 6, 2008, pp. 41-46. (in Japanese)

[19] Z. Jide, W. Zhixin and L. Jude , "The Way to Improve the Trafficability of Vehicles on Sand", *in Proc. 5th European Conf. Terrain-Vehicle Sys.*, Budapest, Hungary, 1991, pp. 121-126.

[20] B.E. Wallace and N.S. Rao, Engineering Elements for Transportation on the Lunar Surface, *Appl. Mech. Rev.*, vol. 46, no. 6, 1993, pp. 301-312.